Transactions of the **13th International Conference on Structural Mechanics in Reactor Technology** (SMiRT 13), Escola de Engenharia - Universidade Federal do Rio Grande do Sul, Porto Alegre, Brazil, August 13-18, 1995

The shape influence on the behaviour of surface cracks

Chawla, D.S., Bhate, S.R., Kushwaha, H.S., Mahajan, S.C.
Bhabha Atomic Research Centre, Reactor Engineering Division, Bombay, India

ABSTRACT: This paper presents the influence of shape of a surface crack on its behaviour under pressure. The J-integral distribution across the axial internal cracks of different shapes in a pressurised pipe has been obtained using line spring method. The results for triangular, circular and rectangular crack shapes are compared to those for elliptical shape.

1 INTRODUCTION

The structural integrity of pressurised components with a surface crack and the estimate of crack growth require the distribution of crack driving force across the crackfront. Though real life cracks tend to have arbitrary shapes or become so after the growth, their idealization into elliptical shape has been largely motivated by availability of exact elasticity solution. ASME code section XI also suggests an enveloping elliptical approximation defined by length and maximum depth of existing crack for evaluation. However the experimental crack growth observations raise questions regarding sensitivity of fracture mechanics results to shape of the cracks. The realistic assessment of the structural integrity of pressurised components thus requires the understanding of the influence of crack shape on its behaviour. This work presents the elasto-plastic behaviour of axial internal surface cracks as influenced by their shapes and geometry parameters under pressure.

The approach uses Line Spring Model(LSM) implemented by Parks (Parks 1981). The basis of the method is to represent the compliance of the ligament by distributed stiffness coupled to plate/shell model of the structure. The stiffness is obtained by considering a Single Edge-Cracked Plate (SECP) under extension and bending forces. The force distribution across the crack is then obtained by numerical solution and it is imposed on SECP to obtain fracture mechanics parameters such as J-integral, crack mouth opening displacement, etc. The method gives satisfactory results for assessment of structural integrity. Incremental plasticity based LSM, available in code (ABAQUS), is used.

2 FINITE ELEMENT MODEL

A straight pipe of 610 mm outside diameter and 50 mm thickness with an internal axial surface crack has been considered for the investigation. One-fourth of the pipe is modelled using eight noded thick shell elements with symmetry boundary conditions at two symmetic planes. Fine mesh is used near crack. Multipoint constraints are used for grading of the element density. The crack is modelled using symmetric line spring elements. Figure 1 shows the mesh near the crack. Line spring elements are shown by dotted lines. The pipe length of approximately 14 times the crack length is modelled to reduce the influence of finite pipe length on the results. The yield strength of the material was 0.1 % of Modulus of Elasticity. Figure 2 shows the different shapes of cracks considered in the analysis.

3 NUMERICAL RESULTS

The finite element model is initially validated by comparing computed peak J-integral values with published (Parks 1982) for an elliptical internal surface crack with depth ratio of 0.5 as shown in figure 3a. The agreement appears to be quite close. The comparison of J-integral values obtained for an external axial elliptical surface with those obtained using three dimensional brick element model (Brocks 1990) is shown in figure 3b. The agreement is satisfactory. LSM results are approx. 20% higher for most of the central portion of crack.

The variation of peak J-integral for different crack shapes obtained by LSM is shown in figure 4a and 4b for shallow and deep crack respectively. The triangular crack appears to produce least driving force while rectangular crack results envelope other results. The differences in J-integral values are negligible during elastic deformation. The differences become significant only after yielding commences. This implies that the crack shape will have strong influence on crack growth and final shape. Approximating a crack by elliptical shape is not conservative approach. However, conservatism is only slightly affected by elliptical approximation. The differences between behaviour of different crack shapes becomes more striking when cracks are deep.

The effect of radius of curvature on the circular geometry for shallow and deep cracks is shown in figure 5a and 5b respectively. The peak J-integral value increases with radius of curvature. As radius increases to large value the results approach those for rectangular crack as they should. The influence of radius of curvature is more predominant for deep crack. The change in the J-integral distribution across the crack front for shallow and deep crack is seen in figure 6a and 6b respectively. The smooth peaked J-distribution becomes more flat with increased radius of curvature for shallow crack. For deep cracks,

however, the flatness of shape reduces with increased radius.

The J-integral values for triangular crack (Figure 7a,7b) show an interesting feature, more prominently for deep crack. The J-integral increases with pressure but peak does not ocuur at centre where depth is maximum. After yielding commences, the peak J-value occurs at approximately x/c = 0.5 and the peak point starts moving towards the centre gradually. The J-value at centre is approximately 20 % less than the peak value for normalized pressure 1.176. This indicates that the initial crack extension will not occur at centre, but away from centre. For a given crack extension normal to the front, the area uncovered by crack will be more for locations away from the centre. Moreover, the normal to the crack front is not uniquely defined at centre of crack. Hence crack extension process may choose locations such that the crack shape becomes smoother after the growth. These features are absent in the J-distribution for rectangular cracks(Figure 8a,8b) and elliptical cracks(Figure 9a,9b).

4 CONCLUSIONS

For an axial internal surface crack in a pipe subjected to internal pressure, the crack driving potential (J-integral) distribution is the characteristic signature of each crack shape after yielding commences in the ligament. Rectangular crack produces maximum driving potential. Though the irregular shape of crack has been considered (ASME) to be analysed with an enveloping elliptical crack, it is not necessary that it is conservative assumption. However, the difference between elliptical and rectangular shape is not significant. For deep circular crack, the radius of curvature strongly influences the J-integral distribution. The peak driving potential for triangular crack does not occur at centre, the point of maximum depth, but slightly away from the centre where a given crack extension will uncover more area of crack front. Thus crack extension process is likely to make the crack smoother.

REFERENCES

ABAQUS.version 5.3. Hibbit,Karlson and Sorenson Associates.

Brocks W. & Kunecke G.1990. Elasto-plastic fracture mechanics analysis of a pressure vessel with an axial outer surface flaw. Nuclear Engg Design.119.307-315.

Parks D.M.1981.The inelastic line spring:Estimates of E.P. fracture mechanics parameter for surface cracked plates and shells.ASME.JPVT.103.246-254.

Parks D.M.& White C.S.1982.Elastic-plastic line spring finite element for surface cracked plates and shells. ASME. JPVT. 104. 1982, 287-292.

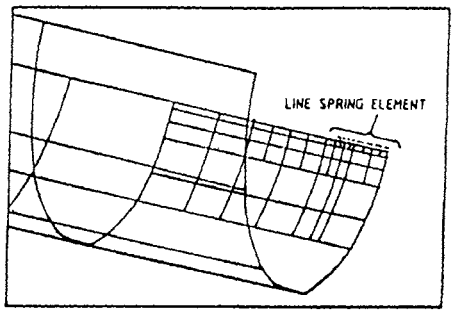

Fig. 1 Finite element mesh near surface crack

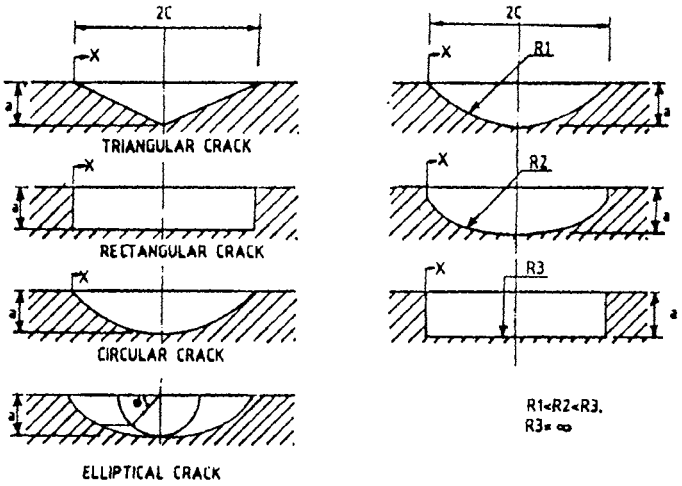

Fig. 2 Different shapes of surface crack

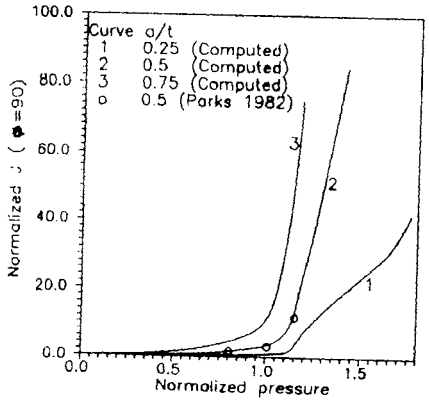

Fig. 3a J-int.($EJ/\sigma_Y^2 t$) vs pressure($pR/\sigma_Y t$) for elliptical crack ($2c/a=6$).

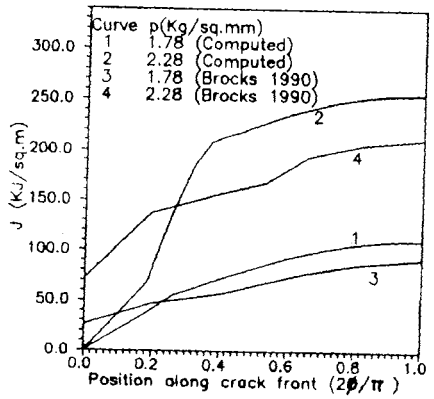

Fig. 3b Comparison of computed J-int. with 3-D results for external axial crack.

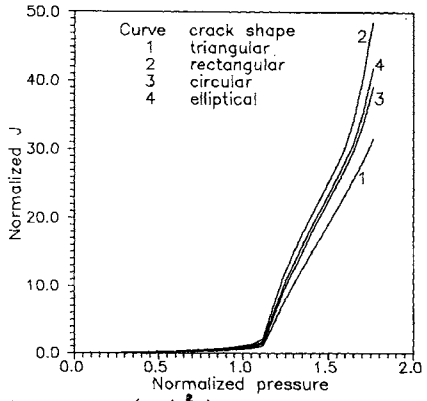

Fig. 4a J-int.($EJ/\sigma_y^2 t$) at centre of crack vs pressure($pR/\sigma_y t$) for different shapes of shallow crack (a/t=0.25, 2c/a=6).

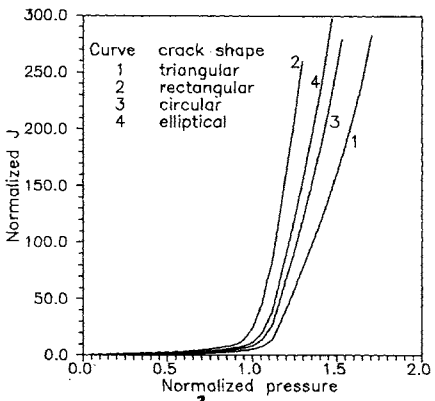

Fig. 4b J-int.($EJ/\sigma_y^2 t$) at centre of crack vs pressure($pR/\sigma_y t$) for different shapes of deep crack (a/t=0.75, 2c/a=6).

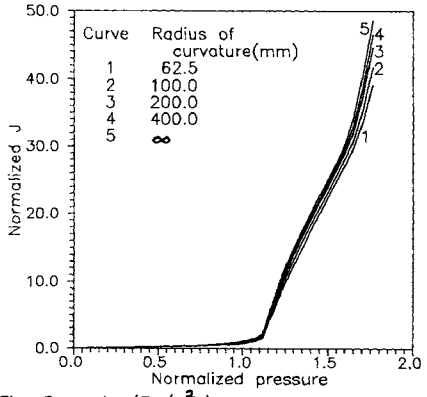

Fig. 5a J-int.($EJ/\sigma_y^2 t$) at centre of crack vs pressure($pR/\sigma_y t$) for shallow circular surface crack (a/t=0.25, 2c/a=6)

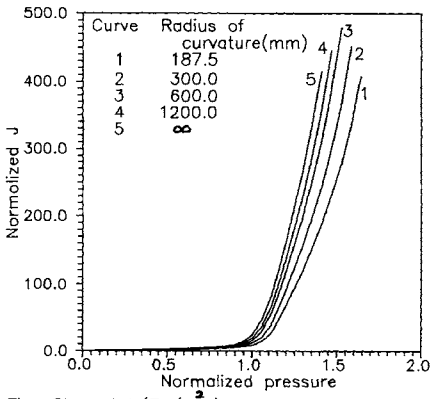

Fig. 5b J-int.($EJ/\sigma_y^2 t$) at centre of crack vs pressure ($pR/\sigma_y t$) for deep circular surface crack (a/t=0.75, 2c/a=6).

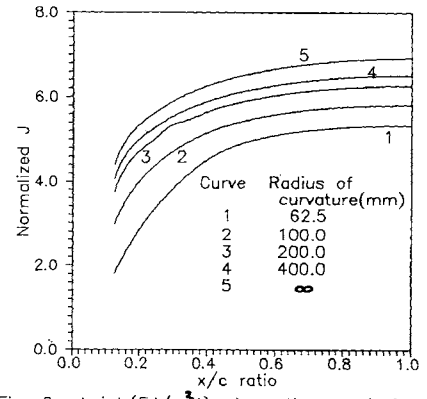

Fig. 6a J-int.($EJ/\sigma_y^2 t$) along the crack front for shallow circular surface crack ($pR/\sigma_y t$=1.176, a/t=0.25, 2c/a=6).

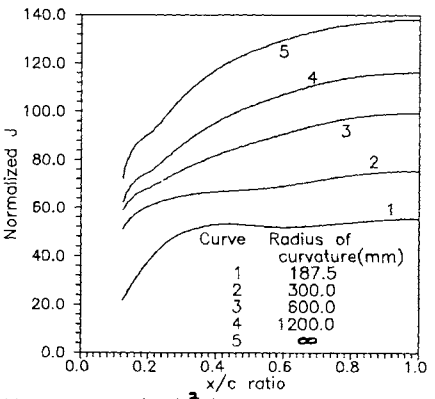

Fig. 6b J-int.($EJ/\sigma_y^2 t$) along the crack front for deep circular surface crack ($pR/\sigma_y t$=1.176, a/t=0.75, 2c/a=6).

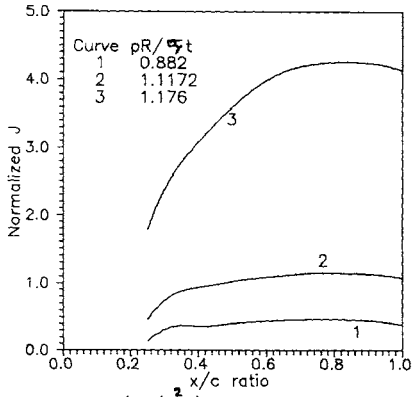

Fig. 7a J-int.($EJ/\sigma_y^2 t$) along the crack front for shallow triangular surface crack (a/t=0.25, 2c/a=6).

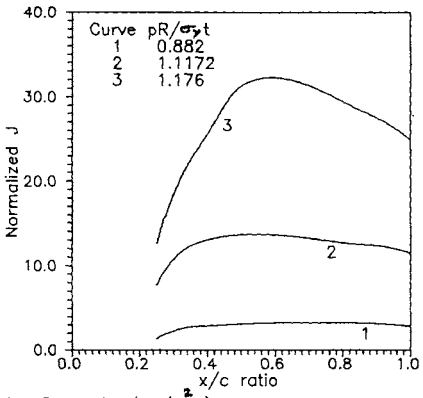

Fig. 7b J-int.($EJ/\sigma_y^2 t$) along the crack front for deep triangular surface crack (a/t=0.75, 2c/a=6)

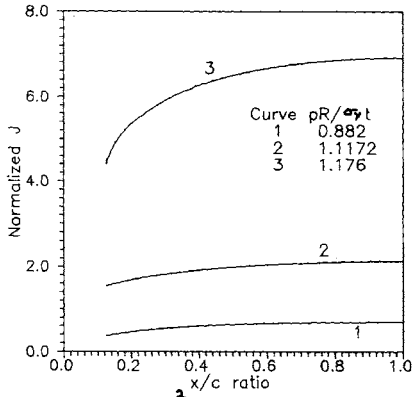

Fig. 8a J-int.($EJ/\sigma_y^2 t$) along the crack front for shallow rectangular surface crack (a/t=0.25, 2c/a=6)

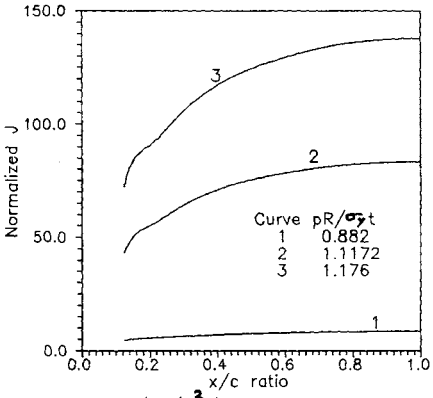

Fig. 8b J-int.($EJ/\sigma_y^2 t$) along the crack front for deep rectangular surface crack (a/t=0.75, 2c/a=6).

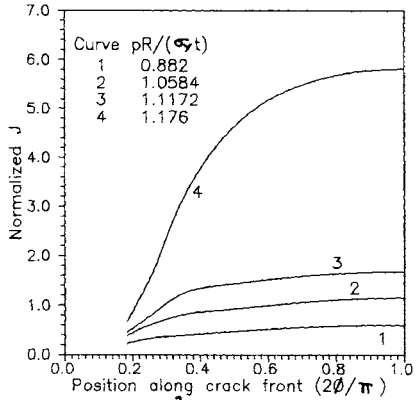

Fig. 9a J-int.($EJ/\sigma_y^2 t$) along the crack front for shallow elliptical surface crack (a/t=0.25, 2c/a=6).

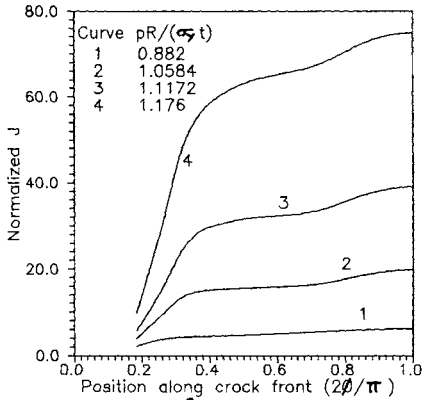

Fig. 9b J-int.($EJ/\sigma_y^2 t$) along the crack front for deep elliptical surface crack (a/t=0.75, 2c/a=6).